

Dynamic Coherence-Based EM Ray Tracing Simulations in Vehicular Environments

Ruichen Wang
ECE department

University of Maryland, College Park
Maryland, USA
rwang92@umd.edu

Dinesh Manocha
CS and ECE department

University of Maryland, College Park
Maryland, USA
dmanocha@umd.edu

Abstract—5G applications have become increasingly popular in recent years as the spread of 5G network deployment has grown. For vehicular networks, mmWave band signals have been well studied and used for communication and sensing. In this work, we propose a new dynamic ray tracing algorithm that exploits spatial and temporal coherence. We evaluate the performance by comparing the results on typical vehicular communication scenarios with NYUSIM, which builds on stochastic models, and Winprop, which utilizes the deterministic model for simulations with given environment information. We compare the performance of our algorithm on complex, urban models and observe the reduction in computation time by 60% compared to NYUSIM and 30% compared to Winprop, while maintaining similar prediction accuracy.

Index Terms—Ray tracing, 5G, mmWave, Vehicular communication.

I. INTRODUCTION

With the rise of mmWave in 5G, many related technologies such as ray tracing (RT) have been studied and updated from sub 6 GHz band to mmWave band. RT can be used in many applications such as field prediction for radio network planning, RT-assist channel estimation for optimal beamforming techniques for mobile backhauling, real-time RT for assisted beamforming, and RT assisted localization [1]. In addition, mmWave has been studied through measurement campaigns for vehicular communications and sensing and showed promising potential at high frequencies [2] [3]. According to [4], the RADar-based COMMunication (RADCOM) technique enables simultaneous communication and sensing, which may further contribute to other technologies. While RADCOM is generating more research interests, ray tracing has been well studied since 1990s. However, dynamic ray tracing is a recently developed idea for performing deterministic ray-based prediction in dynamic environments, where the environment changes or objects in the scenes such as vehicles move. Efficient techniques have been proposed for fast ray tracing in such dynamic environments in sound [5] [6] and visual rendering [7] [8]. It is also gaining more attention with the dramatic increase of mobile devices/users and the advent of wireless systems of traffic control and safety enforcement in the 5G era [9], where the transmitter stays more or less static while the surroundings change. On the other hand, we can also choose to apply ray-based propagation models to vehicular

propagation with moving terminals and scatterers, as described in [10].

In this paper, we present novel algorithms for dynamic ray tracing for EM simulation in large environments, that utilize temporal and spatial coherence, and compare its performance in a typical vehicular environment with results from NYUSIM and Winprop. Our algorithm uses bounding volume hierarchy (BVH) with efficient techniques to recompute or update these hierarchies during each frame [11], and frame-to-frame coherence along with combining path tracing and radiosity methods [12]. Section II discusses related works and briefly introduces selected ray tracing software. Section III shows GDEM details and the simulated environment. Section IV compares and discusses the simulation results. Section V concludes the paper and argues that our novel dynamic ray tracing approach is comparable to both academic and industrial ray tracing simulators and mentions potential future dynamic and real time ray tracing research. The key contributions of this paper are:

- We propose the first dynamic coherence-based ray tracing algorithm at EM bands for fast and reliable RT simulations.
- We develop a new ray tracing software, GDEM, which can work at mmWave frequencies, and show that it speeds up at least 30% in computation time with comparable prediction accuracy to other simulators like NYUSIM and Winprop.
- We specifically perform ray tracing simulations in a typical vehicular communication environment and study the LOS and NLOS performances.

II. RELATED WORK AND AVAILABLE RAY TRACING SOFTWARE

Analysis of potential mmWave solutions to 5G has been conducted worldwide, and many measurements for indoor and outdoor scenes are described in [13] [14] [15]. However, the models built based on site-specific data could suffer significantly when moving to another site [16]. Another approach to building reliable models is an analytical approach, which can achieve high prediction accuracy when the environment is precisely built and computed with refined simulation setups. In our GDEM ray tracing software development process, we

evaluate our results with NYUSIM and Winprop since they are 1) widely used for different scenarios and 2) not very difficult to install, with relatively detailed documents for their theory bases/user manual.

There are other RT software solutions currently in both industry and academia. We provide a brief description of the selected ray tracing software below and summarize the frequency range and applicable scenario in Table I.

Winprop [17] is an RT software from Altair that can support standard RT, Intelligent Ray Tracing (IRT) and Dominant Path models (DPM) at frequencies up to 75 GHz. It is also capable of simulating the spatial variability of the objects in various propagation scenarios.

Wireless Insite [18] developed by Remcom can provide ray tracing coupled with empirical and deterministic models for frequencies up to 100 GHz. It is accelerated by dimension reduction algorithms as well as GPU and multi-threaded CPU hardware acceleration.

NYUSIM [19] is an open-source mmWave channel model simulator developed by NYU Wireless based on years of measurements conducted at various frequencies. It is a generic statistical model that runs fast but does not take in site-specific information.

CloudRT [20] is an academic ray tracing tool created by members of the State Key Laboratory of Rail Traffic Control and Safety at Beijing Jiaotong University. This method is aimed at designing a high-performance cloud-based RT simulation platform that supports frequencies up to 325 GHz, includes all kinds of propagation mechanisms and mobile scattering objects, and is accelerated with a space partitioning algorithm and multi-thread computing.

GEMV² is another academic ray tracing tool developed in [21] to analyze vehicle-to-vehicle channels in large environments [22]. This tool can simulate city-wide networks with tens of thousands of vehicles on commodity hardware, providing hybrid RT along with empirical models. However, this work is based on MATLAB and only evaluated by measurements at 5.9 GHz.

TABLE I
COMPARISON OF COMMERCIAL AND ACADEMIC RT
SIMULATORS

Simulator	Frequency range	Environment
Winprop	up to 75 GHz	Outdoor/indoor
Wireless Insite	up to 100 GHz	Outdoor/indoor
NYUSIM	up to 100 GHz	Outdoor/indoor
CloudRT	up to 325 GHz	Outdoor
<i>GDEM^{V2}</i>	5.9 GHz	Outdoor
GDEM	up to 72 GHz	Outdoor/indoor

III. GDEM AND SIMULATION SCENARIO

Before going into the details of RT algorithms, we first define the concept of a ray in EM simulations. A ray is a high frequency approximation of Maxwell's equations for

propagating EM waves based on the electric and magnetic fields expressions as follows:

$$\vec{E}(\vec{r}) = \vec{e}(\vec{r})e^{-j\beta_0 S(\vec{r})} \quad (1)$$

$$\vec{H}(\vec{r}) = \vec{h}(\vec{r})e^{-j\beta_0 S(\vec{r})} \quad (2)$$

where $\vec{e}(\vec{r})$ and $\vec{h}(\vec{r})$ are magnitude vectors and $S(\vec{r})$ is the optical path length or eikonal. When $\beta_0 \rightarrow \infty$ and considering a series of wavefronts, the power flow lines perpendicular to the wavefronts are the rays and they do not intersect if there is no focus point. Thus, the ray trajectory will be a straight line in a homogenous medium. The detailed mathematical derivation steps can be found in [23]. In conclusion, the ray which helps in analyzing the different propagation mechanisms, is a straight line in a homogenous medium that carries energy and obeys the laws of reflection, transmission, and diffraction. In GDEM, we considered four kinds of rays:

- Direct rays: If a ray goes from the source to the field point directly, the line of sight (LoS) propagation mechanism will be applied, and the pathloss will be simulated by

$$PL(envr, f_c, d)[dB] = FSPL(f_c, d_0 = 1) + n_{envr, f_c} * 10 \log_{10} d + X_\delta(envr, f_c, d)[dB] \quad (3)$$

which is proposed in [15].

- Reflected and transmitted rays: If a ray is reflected or transmitted one or more times before reaching the field point, the ray will be segmented into different parts by reflected or transmitted points and be applied with the directed path loss model for each segment. The study in [1] shows that at the mmWave band, the signal power will be negligible at a high order of reflections and transmissions. In this proposed RT tool, the reflection/transmission time is set to 10 to balance the running time and accuracy by simulations trials.
- Diffracted rays: The diffracted rays are more complicated than the two types of rays mentioned above, since one incident ray at the geometry edge can lead to a cone of diffracted rays. The uniform theory of diffraction (UTD) [24] is applied to calculate the diffraction coefficients here and the detailed steps are followed as described in [25]. The upper bound of diffraction time simulated is set to 3 in this tool by practice.
- Diffused and scattered rays: The last type of rays comes from rough surfaces such as building exteriors. The scattered rays will be divided into specular and nonspecular components and simulated by the effective roughness model suggested in [23] [26].

In addition to ray simulation, we also performed the phase calculation.

For the acceleration methods, GDEM utilized three main algorithms: backward ray tracing from the receiver in the visibility determination step, the use of BVH and minimizing its rebuilding cost between frames, and the propagation path caching for better frame coherence [21].

- *Backward ray tracing*: In the backward RT algorithm, rays are cast from the listener, rather than from each

source. It was observed that the early reflections and diffractions that contribute more to the total received power tend to come from geometry in the vicinity of the receiver. In fact, when casting rays from the source, only a few may reach the receiver and may not be the most perceptually important paths, resulting in more rays to be cast to get necessary propagation paths. The backward RT method can get all the important paths while shooting fewer rays. The backward RT strategy also benefits from the fact that the amount of rays no longer scales linearly with the number of sources.

The brief process is as follow: 1) cast a random sphere of sampled rays, 2) record reflections and keep a hash table of visited propagation paths for each depth of reflection (up to a user defined threshold, 10 in GDEM), 3) generate a series of image receiver positions when encountering a new triangle series, 4) check the source if there is a valid path to the receiver, 5) if any edge marked as diffraction edge, consider the sources that lie in the diffraction shadow region from the receiver’s perspective, and use the UTD diffraction formulation to determine the point on the edge at which diffraction occurs and then perform path validation back to the receiver as with reflection paths, 7) for each valid propagation path, the system calculates the total distance along the path, the direction of the path from the receiver, and the total attenuation and phase distortion along the path.

- *Efficient BVH updating:* BVHs have been widely used to accelerate the performance of ray tracing algorithms [27], and we take one step further to efficiently recompute or update these hierarchies during each frame, for that the rebuilding of BVHs is expensive in practice, and we minimize the cost by measuring BVH quality degradation between successive frames. The advantages of our method are: 1) it will update/rebuild at a time when necessary without any scene specific settings, 2) when there is little to no degradation, the rebuild would not be initiated, and 3) it is possible to just rebuild subtrees in some cases. These help improving the system computation efficiency and detailed evaluations can be found in [11].
- *Propagation path caching:* The visibility hash tables as persistent caches are used to accelerate the path finding process from frame to frame. Once the valid paths are found, they are kept and updated until removed, i.e., at the beginning of each frame simulation, all triangle sequences in the hash tables are checked to see if the previous paths are still valid, since the positions of source and receiver do not change much between frames. This method has significantly lowered the number of visibility rays cast each frame, leading to a higher overall frame rate and lower latency for real time applications. More details are described in [28] [29].

For the input, GDEM can take the environment description files including an “.obj” file for the geometry and an “.mtl”

file for the material information in the environment. We use the modeled small European town built by Turbosquid [30] to performed RT simulations. We consider both LOS and NLOS links in vehicular communication as suggested in [4].



Fig. 1. Modeled 3D European village from Turbosquid. We show that our method works better than other simulators in such urban environment, with high accuracy and fast computation time.

IV. RESULTS COMPARISON AND DISCUSSION

We show some selected comparison results in this section. NYUSIM generates power delay profiles (PDP) while Winprop outputs heatmaps of received signal powers (RSP). The NYUSIM results are compared for outdoor vehicular communication scenarios and the Winprop results are compared for indoor scenes to show the prediction accuracy of GDEM.

A. Power Delay Profile Comparison

The vehicle placement and link specifications are shown in the following figure. C2 communicates with C1 and C3 in LOS links, while C1 and C3 has NLOS links.

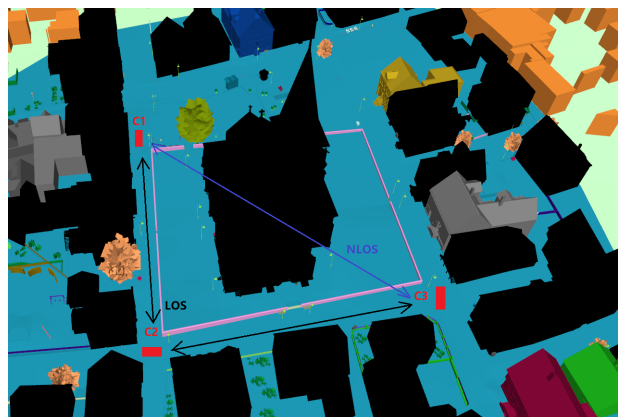


Fig. 2. Typical vehicular communication LOS and NLOS links, screenshot captured by SketchUp. We perform ray tracing simulations in such environment and compare PDPs from NYUSIM and GDEM. The selected results are shown below and more comparisons can be found in the Appendix.

The following figures shows the PDP calculated by NYUSIM and GDEM for LOS and NLOS links.

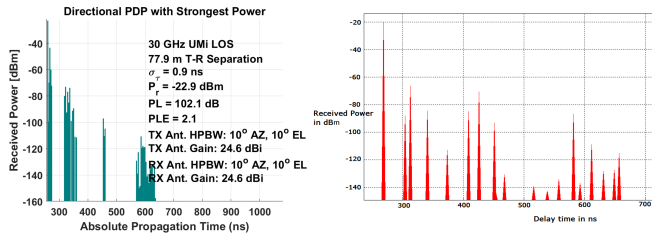


Fig. 3. NYUSIM and GDEM LOS PDP: with the direct path received power -22.95dBm at 259.5ns from NYUSIM and -20.2dBm at 260ns from GDEM, we see similar clustering effects of the subpaths, and GDEM can calculate more paths with longer delay times.

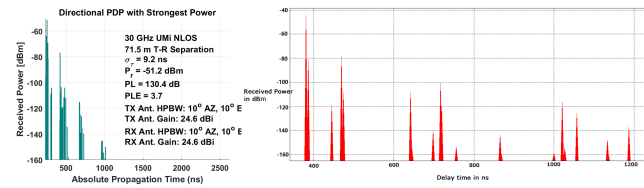


Fig. 4. NYUSIM and GDEM NLOS PDP: there is no direct path in NLOS, the highest RSP in NYUSIM is -51.2dBm and -44.5dBm in GDEM. The overall received power strength is reduced in NLOS scenario. Since GDEM does catch environment information, it can find valid paths with even longer delays.

The simulation parameters of NYUSIM is noted in the plots. We see the PDPs from both simulators share similar behaviors in direct path arrival times (the first arrived signal from direct path has the same delay time) and clustering effects (the PDPs have similar subpath components). GDEM calculated the received power from more resources and showed received powers beyond 200 meters (which corresponds to signals propagating for about 700 ns in delay time).

B. Predicted Received Power Comparison

We perform comparison simulations for indoor environments of Winprop and GDEM, as shown in Fig. 5 of Winprop and GDEM. The signal frequency was set to 30GHz and the TX height is set at 2 meters. The indoor environment consists of walls, doors, and windows with different reflection/transmission/diffraction coefficients, as shown in the following pictures.

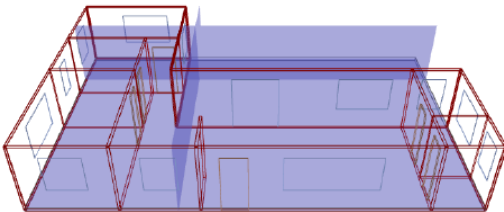


Fig. 5. Simple indoor office environment: we compare the performances of Winprop and GDEM indoor because Winprop took very long time to load and convert the modeled village environment shown in Fig. 1. This indoor environment with known material information is easy to use for prediction accuracy and performance validation.

The output one-shot heatmaps of the indoor environment by Winprop and GDEM are shown in Fig. 6 and Fig. 7. We see from the two heatmaps that GDEM predictions show behaviors similar to Winprop results. There is, however, some blurred prediction area towards the boundary of the environment, which might be resulting from different boundary condition settings.

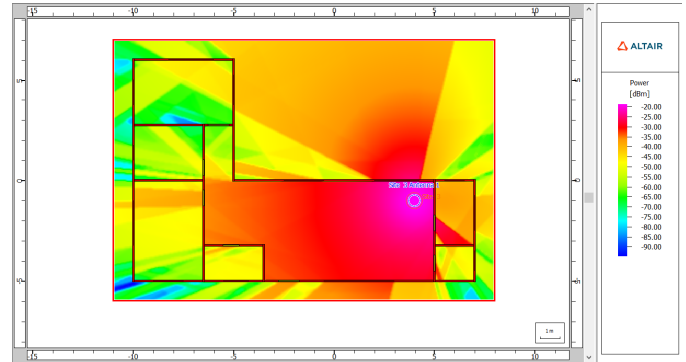


Fig. 6. Received power heatmap by Winprop, using COST351 model at 30GHz for RT simulation suggested by the software manual for balanced accuracy and running time. The color bar on the right indicates the strength of received powers. We see some parts the rays are limited into a cone shape propagation where they are the positions of windows or doors of the office. The material information of walls/doors/windows is provided by Winprop.

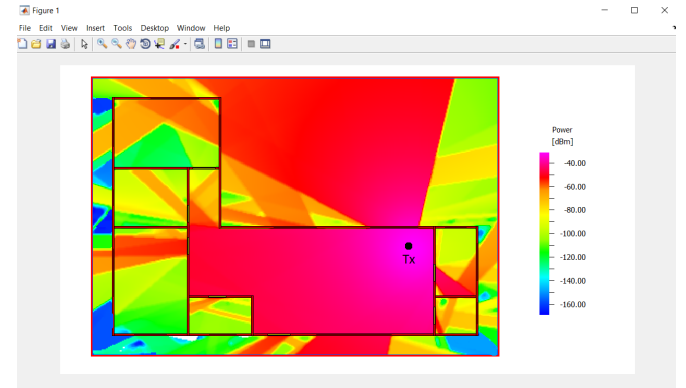


Fig. 7. Received power heatmap by GDEM, using the discussed models for predictions at 30 GHz. The same environment and material information is encoded. We can clearly see the reflection at walls, diffraction at edges, and transmission through windows/walls. Due to the model difference, we see the details of two heatmap are slightly different while the ray behaviors are similar. The accuracy comparison is shown by prediction difference histogram in Fig. 9

A total of three testing cases were simulated with different Tx locations. The other two pairs of comparison heatmaps are shown below with different TX locations in the environment (see Fig. 8).

The histogram of the difference between the predicted heatmaps from Winprop and GDEM is shown below. According to the numbers, about 70.1% of the prediction difference is 0, 86.6% of the prediction difference is less than 40%, and 74.5% of the prediction difference with less than 5%

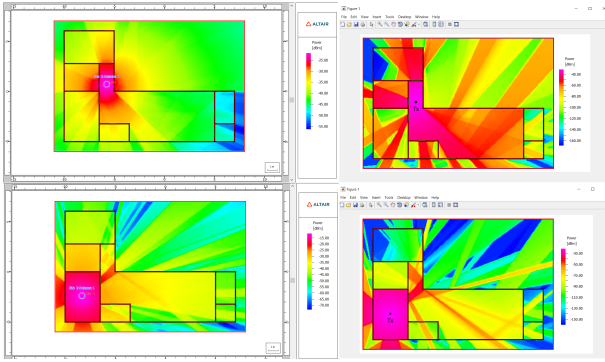


Fig. 8. More received power heatmaps by Winprop (left) and GDEM (right) for indoor environment with different TX locations. This shows that our method is valid for this whole indoor environment with comparable accuracy to Winprop.

difference. Another figure shows the histogram excluding difference zero.

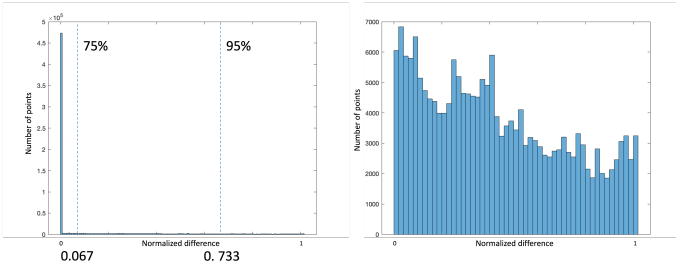


Fig. 9. Histogram of normalized prediction difference between Winprop and GDEM in TX location 1 as Fig. 6, w/ and w/o zero difference points, the 75% and 95% percentiles are marked in the plot. Over 70% predictions are the same between Winprop and GDEM

C. Runtime Comparison

We summarize the working time of the simulations in the following tables. The parameter settings of the comparison between NYUSIM and GDEM are: 10 Rx locations run in NYUSIM and 2000 shooting rays without computing reflections/diffractions/transmissions. In Table II we see that the GDEM is faster when computing only the direct paths.

Table III shows the comparison between Winprop and GDEM

TABLE II
RUNNING TIME COMPARISON OF NYUSIM AND GDEM

Simulator	Runtime case1	Runtime case2	Runtime case3
NYUSIM	40s	42s	40s
GDEM	15s	16s	16s

with the whole simulation process, including reading in the modeled village file. Winprop takes a longer time. When taking only the ray tracing simulation time into consideration or performing ray tracing in a simple indoor environment, we set the parameters as follow: Winprop resolution range 0.02m, and takes max 2 reflections, 2 transmissions, and 1

diffraction, by 3d ray tracing model, while GDEM runs with 2000 shooting rays, max 2 reflections, 2 transmissions, and 1 diffraction, Table IV shows that Winprop has a slightly better, but similar computation time to GDEM.

TABLE III
RUNNING TIME COMPARISON OF WINPROP AND GDEM

Simulator	Runtime test1	Runtime test2
Winprop	60min	65min
GDEM	45min	42min

TABLE IV
RUNNING TIME COMPARISON OF WINPROP AND GDEM EXCLUDING ENVIRONMENT INPUT PROCESSING

Simulator	Runtime case1	Runtime case2	Runtime case3
Winprop	26s	25s	29s
GDEM	30s	31s	35s

V. CONCLUSION

In this paper, we proposed a reliable and fast RT simulator at EM bands for a typical vehicular communication scenario with a novel dynamic ray tracing algorithm that exploits spatial and temporal coherence. We performed simulations to compare our method with two other RT simulators from academia and industry. The Ericsson's 5G demo from a recent NVIDIA Omniverse keynote speech [31] showed a ray tracing simulation between base stations and vehicles in a complex environment in the air. Therefore, our next step will be to upgrade the GDEM to perform RT simulations in a more complex and dynamic environments in real time.

REFERENCES

- [1] Fuschini, Franco, et al. "Ray tracing propagation modeling for future small-cell and indoor applications: A review of current techniques." *Radio Science* 50.6 (2015): 469-485.
- [2] Ben-Dor, Eshar, et al. "Millimeter-wave 60 GHz outdoor and vehicle AOA propagation measurements using a broadband channel sounder." 2011 IEEE Global Telecommunications Conference-GLOBECOM 2011. IEEE, 2011.
- [3] Samimi, Mathew K., and Theodore S. Rappaport. "3-D millimeter-wave statistical channel model for 5G wireless system design." *IEEE Transactions on Microwave Theory and Techniques* 64.7 (2016): 2207-2225.
- [4] Lübke, Maximilian, et al. "Comparing mmWave Channel Simulators in Vehicular Environments." 2021 IEEE 93rd Vehicular Technology Conference (VTC2021-Spring). IEEE, 2021.
- [5] Schissler, Carl, and Dinesh Manocha. "Interactive sound rendering on mobile devices using ray-parameterized reverberation filters." *arXiv preprint arXiv:1803.00430* (2018).
- [6] Manocha, Dinesh, and Ming C. Lin. "Interactive sound rendering." 2009 11th IEEE International Conference on Computer-Aided Design and Computer Graphics. IEEE, 2009.
- [7] J. Burgess, "RTX on—The NVIDIA Turing GPU," in *IEEE Micro*, vol. 40, no. 2, pp. 36-44, 1 March-April 2020, doi: 10.1109/MM.2020.2971677.
- [8] Steven G. Parker, James Bigler, Andreas Dietrich, Heiko Friedrich, Jared Hoberock, David Luebke, David McAllister, Morgan McGuire, Keith Morley, Austin Robison, and Martin Stich. 2010. OptiX: a general purpose ray tracing engine. *ACM Trans. Graph.* 29, 4, Article 66 (July 2010), 13 pages. DOI:https://doi.org/10.1145/1778765.1778803

- [9] Bilibashi, D., E. M. Vitucci, and V. Degli-Esposti. "Dynamic ray tracing: Introduction and concept." 2020 14th European Conference on Antennas and Propagation (EuCAP). IEEE, 2020.
- [10] Azpilicueta, Leyre, Cesar Vargas-Rosales, and Francisco Falcone. "Intelligent vehicle communication: Deterministic propagation prediction in transportation systems." IEEE Vehicular Technology Magazine 11.3 (2016): 29-37.
- [11] Lauterbach, Christian, et al. "RT-DEFORM: Interactive ray tracing of dynamic scenes using BVHs." 2006 IEEE Symposium on Interactive Ray Tracing. IEEE, 2006.
- [12] Schissler, Carl, Ravish Mehra, and Dinesh Manocha. "High-order diffraction and diffuse reflections for interactive sound propagation in large environments." ACM Transactions on Graphics (TOG) 33.4 (2014): 1-12.
- [13] Rappaport, Theodore S., et al. "Millimeter wave mobile communications for 5G cellular: It will work!." IEEE access 1 (2013): 335-349.
- [14] Degli-Esposti, Vittorio, et al. "Measurement and modelling of scattering from buildings." IEEE Transactions on Antennas and Propagation 55.1 (2007): 143-153.
- [15] MacCartney Jr, George R., et al. "Millimeter wave wireless communications: New results for rural connectivity." Proceedings of the 5th workshop on all things cellular: operations, applications and challenges. 2016.
- [16] Nguyen, Huan Cong, et al. "Evaluation of empirical ray-tracing model for an urban outdoor scenario at 73 GHz E-band." 2014 IEEE 80th Vehicular Technology Conference (VTC2014-Fall). IEEE, 2014.
- [17] Winprop <https://www.altair.com/feko-applications/>
- [18] Wireless Insite <https://www.remcom.com/wireless-insite-emp-propagation-software/>
- [19] Sun, Shu. Nyusim user manual." New York University and NYU WIRELESS (2017).
- [20] CloudRT <http://cn.raytracer.cloud/>
- [21] M. Boban, J. Barros, and O. K. Tonguz, "Geometry-based vehicle-to-vehicle channel modeling for large-scale simulation," IEEE Trans. Veh. Technol., vol. 63, no. 9, pp. 4146-4164, Nov. 2014.
- [22] *GEMV*² <http://vehicle2x.net/>
- [23] Yun, Zhengqing, and Magdy F. Iskander. "Ray tracing for radio propagation modeling: Principles and applications." IEEE Access 3 (2015): 1089-1100.
- [24] Kouyoumjian, Robert G., and Prabhakar H. Pathak. "A uniform geometrical theory of diffraction for an edge in a perfectly conducting surface." Proceedings of the IEEE 62.11 (1974): 1448-1461.
- [25] Balanis, Constantine A. Advanced engineering electromagnetics. John Wiley & Sons, 2012.
- [26] Hossain, Ferdous, et al. "An efficient 3-D ray tracing method: prediction of indoor radio propagation at 28 GHz in 5G network." Electronics 8.3 (2019): 286.
- [27] Smits, Brian. "Efficiency issues for ray tracing." Journal of Graphics Tools 3.2 (1998): 1-14.
- [28] Schissler, Carl, and Dinesh Manocha. "Gsound: Interactive sound propagation for games." Audio Engineering Society Conference: 41st International Conference: Audio for Games. Audio Engineering Society, 2011.
- [29] Rungta, Atul, et al. "Diffraction kernels for interactive sound propagation in dynamic environments." IEEE transactions on visualization and computer graphics 24.4 (2018): 1613-1622.
- [30] <https://www.turbosquid.com/>
- [31] <https://blogs.nvidia.com/blog/2021/11/09/ericsson-digital-twins-omniverse/>

VI. APPENDIX

We showed more LOS and NLOS comparisons from NYUSIM and GDEM here. The following figures show the environment setups and the simulation results from NYUSIM Fig. 11 - Fig. 12 and from GDEM Fig. 13 - Fig. 14. These results showed that the proposed algorithm works well with moving object in urban environment. Our future work will be simulating more complex scenes with more moving objects and complex building blocks.

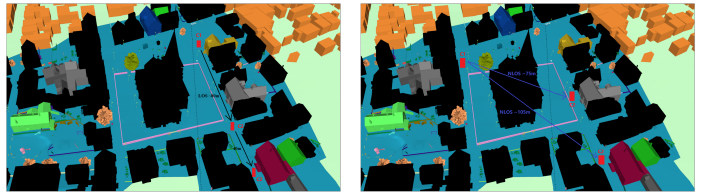


Fig. 10. Typical vehicular communication LOS and NLOS links with extended ranges, approximated distances specified in the figures.

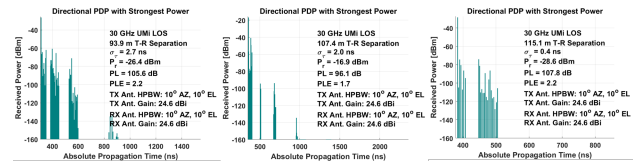


Fig. 11. NYUSIM LOS PDP from 93m to 115m, however, since NYUSIM does not take in the environment information, and thus the distance change can not track the moving vehicle.

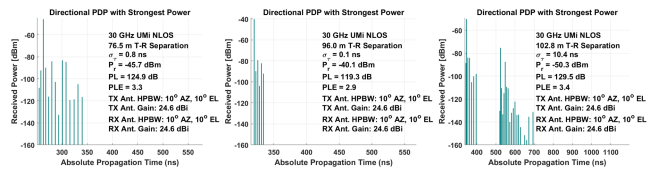


Fig. 12. NYUSIM NLOS PDP from 93m to 115m, we see NLOS scenario does experience more path loss, but does not impact the multipath propagation.

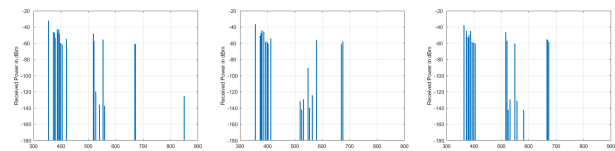


Fig. 13. GDEM LOS PDP from 80m to 100m, we see the decreased direct path received power and longer delay as the car moving away, and the clustering of subpaths changed consistently.

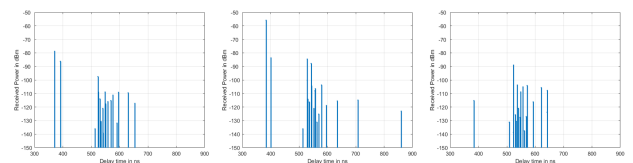


Fig. 14. GDEM NLOS PDP from 75m to 105m, we see the overall reduced power and the PDPs are very different at each step according to the environment change as the car moving in NLOS. However, we see the main cluster of subpaths at 500-600ns which suggests that the common valid paths are recorded and thus saves the computation resources.